J Appl Electrochem (2008) 38:515–522
DOI 10.1007/s10800-007-9466-2

ORIGINAL PAPER

Immobilization of dendrimer-encapsulated platinum nanoparticles on pretreated carbon-fiber surfaces and their application for oxygen reduction

**J. Ledesma-García · I. L. Escalante García ·
Francisco J. Rodríguez · Thomas W. Chapman ·
Luis A. Godínez**

Received: 16 July 2007 / Revised: 29 November 2007 / Accepted: 29 November 2007 / Published online: 14 December 2007

Abstract This paper reports the successful preparation of catalytic electrodes based on carbon-fiber paper modified with dendrimer-encapsulated platinum nanoparticles. The metallic nanoparticles were first synthesized from solution within generation-four hydroxyl-terminated PAMAM dendrimers, which serve as a carrier for their subsequent immobilization on the solid substrates. The carbon-fiber surfaces were activated by means of three alternative anodic pretreatments and then loaded with the dendrimer-metal nanocomposites by cycling of the carbon-electrode potential. The degree of oxidation of the carbon surface affects the anchoring of the dendritic material, the coverage of which is indicated by the electroactive area of the encapsulated platinum. The modified carbon-fiber surfaces pretreated by cyclic polarization are found to be electrocatalytic for the oxygen reduction reaction, presenting a good exchange-current density at low platinum loading.

Keywords Carbon-fiber electrodes · PAMAM dendrimers · Platinum nanoparticles · Oxygen reduction

1 Introduction

Because of their physical, chemical and electrochemical properties, such as good electrical and thermal conductivities, low density, corrosion resistance, and low elasticity, carbon materials are used extensively in a wide variety of electrochemical systems. Carbon can be produced in a great variety of forms that are readily available and generally of low-cost. These forms are used as electrodes, structural components, or conductive supports of electrocatalysts in batteries and fuel cells and for analytical applications [1–8].

Carbon-fiber is an attractive material for application as a fuel-cell electrode because of its flexibility, durability and high surface area. The hydrophobic and less reactive character of the carbon-fiber, however, restricts its surface modification, which is needed to enhance its catalytic activity [9]. Some pretreatment is usually necessary for the modification of carbon surfaces [10, 11]. Several oxidation methods have been developed as pretreatments, including both chemical oxidation [12–14] and electrochemical oxidation in aqueous and other media [9, 15].

For electrochemical activation of a carbon surface a number of possibilities exist, such as galvanostatic, potentiostatic or cyclic polarization in various electrolytes [16]. Electrochemical oxidation of carbon-fibers, in particular, may provide a way of activating the surface through changes in the morphology as well as increasing the coverage by various oxygen-containing functional groups, such as quinone, carboxylic, anhydride or lactone species [2, 9, 17–19]. These functional groups serve as anchors for preparing modified electrodes for analytical or other catalytic purposes.

Maeda et al. [20–23] have reported extensive work on the covalent modification of glassy-carbon electrodes for analytical purposes by linking alkanol molecules via an ether linkage produced by electrochemical oxidation in acid media. On the basis of their work, Ye et al. [24, 25] recently developed a strategy for grafting dendrimer-encapsulated platinum nanoparticles to glassy-carbon

---

J. Ledesma-García · I. L. Escalante García ·
F. J. Rodríguez · T. W. Chapman · L. A. Godínez (✉)
Department of Electrochemistry, Centro de Investigación y Desarrollo Tecnológico en Electroquímica, Parque Tecnológico Querétaro, Sanfandila, Pedro Escobedo, CP 76703 Queretaro, Mexico
e-mail: lgodinez@cideteq.mx

electrodes by cycling the potential. The resulting electrodes were studied from the point of view of their catalytic properties.

Dendrimer-metal nanocomposites in solution are prepared by absorbing metallic ions into hydroxyl- or amine-terminated poly(amidoamine) (PAMAM) dendrimers where they are complexed with interior amine groups. After their absorption, chemical reduction of the metal ions yields dendrimer-encapsulated metal nanoparticles [26–29]. The ability to control nanoparticle size and composition makes these [30–33] as well as other templating materials [34] extremely attractive for use as supported catalysts.

The primary objective of this work was to examine the preparation of activated carbon-fiber electrodes that might be used as fuel cell cathodes for oxygen reduction. We investigated the effects of surface oxidation of the carbon fibers on the anchoring of hydroxyl-terminated dendrimers that encapsulate platinum nanoparticles (G4OHPt) and compared several alternative pretreatment methods. Figure 1 illustrates the electrode preparation and modification procedures. The surfaces of carbon-fiber were first functionalized by means of three alternative electrochemical pretreatments in acidic media for the purpose of obtaining activated surfaces bearing oxidized groups of varying characteristics (Step 1). Then platinum-dendrimer nanocomposites were incorporated following the method of Ye and coworkers [24, 25] (Step 2). Electrochemical studies confirmed the presence of platinum nanoparticles on the porous carbon material as well as their catalytic activity for the oxygen-reduction reaction.

2 Experimental

2.1 Materials

Carbon-fiber electrodes were constructed using Toray® paper (0.19 mm thick). In the pretreatment and modification processes, circular disks of the carbon paper, 0.6 cm in diameter, were exposed to the solutions. Generation-4 hydroxyl-terminated PAMAM dendrimers (G4OH) with the highest available purity (10 wt% in methanol) were obtained from Aldrich and used without further purification. Platinum nanoparticles were prepared from K_2PtCl_4 (Strem Chemicals) by reduction with $NaBH_4$ (J. T. Baker). The electrolyte solutions for electrochemical experiments consisted of 0.1 M NaF or 0.5 M H_2SO_4 (J. T. Baker). All aqueous solutions were prepared using deionized water ($\rho \geq 18$ MΩ cm). Research-grade N_2 and O_2 gases were purchased from Infra and Praxair respectively (both 99.999% pure).

2.2 Synthesis and characterization of G4OHPt

Fourth-generation hydroxyl-terminated poly(amidoamine) dendrimers (G4OH) were used to prepare dendrimer-encapsulated Pt nanoparticles according to the reported procedures [35]. The concentration of the platinum salt in water was 6 mM, and the molar ratio between the metal-bearing ion and the dendrimer was 60:1. The mixture was stirred for 48 h with the purpose of forming a complex

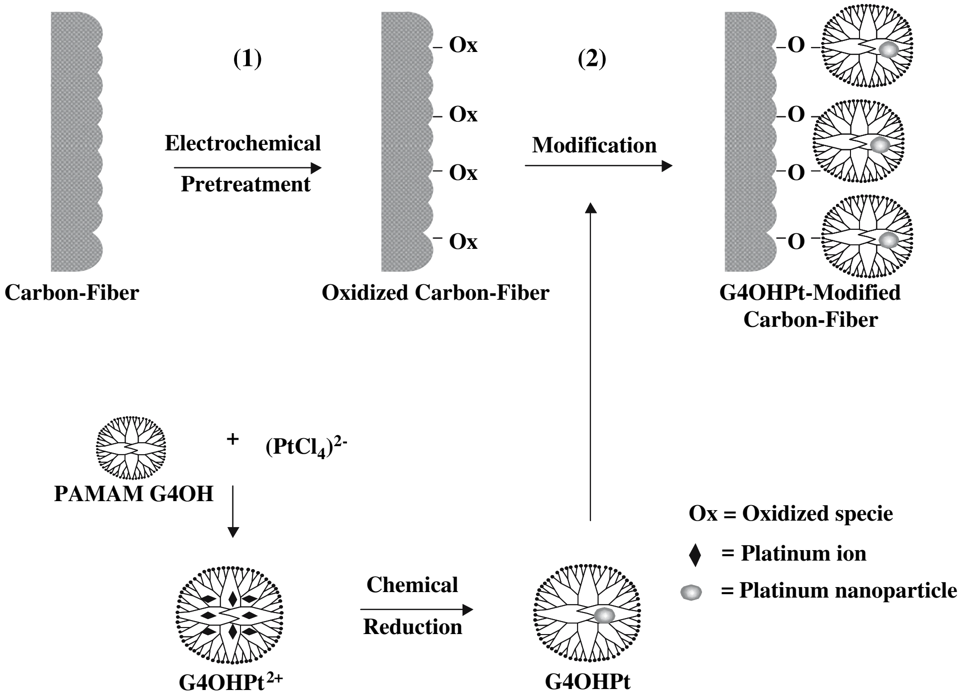

Fig. 1 Schematic representation of the carbon-fiber functionalization and modification procedures. Step 1 involves the activation of the surface by means of different electrochemical treatments. Step 2 is the modification of the pretreated carbon fiber by scanning of potential in a solution of previously synthesized dendrimer-encapsulated nanoparticles

between interior tertiary amine groups of PAMAM G4OH and platinum ions, which was monitored by UV–Vis spectroscopy with an Agilent Model 8453 UV–vis spectrophotometer offering spectral resolution of 2 nm, using quartz cells with 10 mm path length. A ligand-to-metal charge-transfer (LMCT) band attributed to the Pt-dendrimer complex appears at 250 nm [28]. The observed response was comparable to published data [28, 36]. Subsequently, metallic Pt nanoparticles (G4OHPt) were obtained by reducing the Pt-dendrimer complex through addition of an excess of aqueous 0.5 M $NaBH_4$ solution and stirring for 24 h. Finally, the G4OHPt was purified by dialysis using benzoylated cellulose-membrane tubing (Sigma-Aldrich) having a cut-off of 1,200 Da [37].

X-ray diffraction (XRD) patterns obtained with films of G4OHPt deposited by solvent evaporation onto Si substrates using a Philips X-Pert 3710 diffractometer confirmed the presence of metallic Pt. The particle size was calculated by use of the Scherrer equation [38] and confirmed via SEM analysis carried out on G4OHPt-modified carbon fibers with a Philips XL 30 scanning electron microscope.

2.3 Functionalization of carbon-fiber electrodes by anodic pretreatment

All the electrochemical experiments were performed using an Epsilon potentiostat, Version 1.40.67, from Bioanalytical Systems. Carbon-fiber disks (0.6 cm diameter) were treated as working electrodes in a standard three-electrode glass cell, using a mercury/mercurous sulfate reference electrode and a Pt wire counter electrode. Three alternative electrochemical pretreatments were conducted in aqueous H_2SO_4 (0.5 M): (1) Cyclic polarization (CP) with 10 cycles between + 1,000 to −1,000 mV at 50 mV s^{-1}; (2) Anodic polarization (AP) at + 1,500 mV for 30 min.; and (3) AP followed by the CP (AP + CP). Potentials are reported here relative to the reference electrode uses unless indicated otherwise. A carbon-fiber electrode without pretreatment (WEP) was used as an experimental control in subsequent tests.

2.4 Modification of the pretreated carbon-fiber electrodes

Modification of previously functionalized carbon-fiber surfaces with G4OHPt was carried out by scanning the carbon potential at 10 mV s^{-1} between 0 and + 1,000 mV [21–24] in aqueous 0.1 M NaF + 40 μM G4OHPt. Ag/AgCl (3 M NaCl) was used as the reference electrode here, and the counter electrode was a platinum wire. The concentration of the G4OHPt was calculated assuming that all of the original G4OH was loaded with Pt and that all of the product was retained in the dialysis treatment.

3 Results and discussion

3.1 Characterization of the dendrimer-encapsulated Pt nanoparticles

The XRD analysis of the electrocatalysts showed a very high degree of crystallinity and the existence of an fcc metallic phase with an average particle size of 2.7 nm. Line-broadening analysis of the primary XRD peak [111] was conducted using the Scherrer treatment of the data [38]. The resulting lattice parameter showed a value of 3.9207, which corresponds closely to that reported for other Pt-based electrocatalysts [39].

3.2 Electrochemical characterization of the pretreated and modified surfaces

Carbon-fiber surfaces functionalized by means of the three alternative electrochemical methods described previously were subjected to several electrochemical tests prior to modification with G4OHPt. Relative surface capacitance values for the three specimens and the carbon-fiber control (WEP) were determined by observing the background currents produced by cyclic voltammetry in sulfuric acid at several scan rates between 10 and 50 mV s^{-1}. A narrow potential range (±50 mV from open-circuit potential, E_{oc}) was used to minimize the contribution of faradaic currents [2, 40]. From the currents observed in the anodic and cathodic scans in the CVs, the capacitance C at E_{oc} was calculated from the CV data using the relation, $C = i/v$, where i and v are the current and the scan rate, respectively [41]. The relative values of surface capacitance are shown in Fig. 2. The relative capacitance values depend of the method of activation, which could be related directly to the formation of various oxidized groups on the surface that increase double-layer capacitance. Figure 2 indicates that the surface pretreated by CP alone exhibited lower capacitance than that exposed to the longer-term anodic polarization (AP) and barely more than the untreated material.

Cyclic voltammetry in aqueous H_2SO_4 (0.5 M) confirmed the presence of metallic platinum on the modified carbon-fibers. Figure 3 compares the electrochemical responses of three carbon-fiber electrodes functionalized by means of CP in acid media. Curve *i* corresponds to unmodified carbon-fiber, and curve *ii* represents an electrode modified with only G4OH dendrimer, while

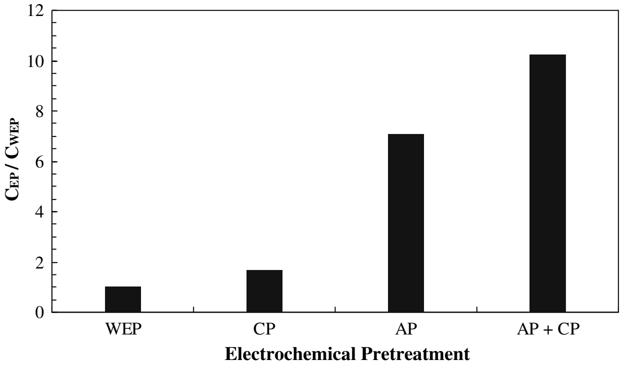

Fig. 2 Variation of the relative surface capacitance with the method of oxidative pretreatment. C_{EP} is the capacitance of the pretreated carbon-fiber electrodes (F g^{-1}), and C_{WEP} is the capacitance of the untreated carbon-fiber (F g^{-1})

curve *iii* gives the response with the G4OHPt composite on the surface. Voltammogram *iii* shows hydrogen adsorption and desorption peaks occurring at the more cathodic potentials as well as the formation and reduction peaks of platinum oxide [42–44] as well as those of superficial groups on the carbon-fiber surface [45], which occur in the same range of potential.

The electroactive area of the Pt nanoparticles encapsulated in the PAMAM dendrimer anchored on the carbon-fibers was determined from the charge attributed to the desorption of one hydrogen atom per Pt site, which for a polycrystalline Pt surface amounts to approximately 210 μC cm^{-2}. The area under the desorption peak was estimated in the region prior to evolution of molecular hydrogen and adjusted by subtraction of the double-layer charging current [46–48]. The charges passed during each method of electrochemical pretreatment were also calculated. The cathodic currents in the surface-reduction peak were integrated to obtain the surface charge density. A baseline correction for capacitance was applied in the case of CP pretreatment. The resulting charge densities should reflect the number of functional groups formed on the carbon support during the oxidation process in each case. Figure 4 presents the surface-charge densities (Q) generated by pretreatment and the electroactive area (A_e) of the dendrimer-encapsulated Pt obtained with each method of pretreatment as well as values for the control. These surface-charge densities are based on the superficial area of the carbon-fiber.

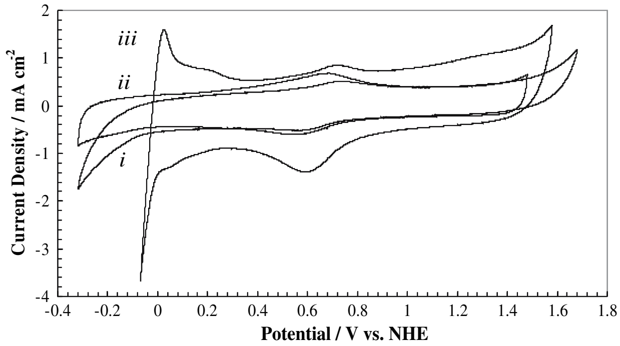

Fig. 3 Cyclic voltammograms of CP-pretreated carbon-fiber electrodes in N_2-purged 0.5 M H_2SO_4: (*i*) unmodified, (*ii*) modified with G4OH and (*iii*) modified with G4OHPt. Scan rate: 50 mV s^{-1}

According to the results shown in Fig. 4, the anodic polarization (AP) pretreatment methods increased the density of oxidized groups on the surface compared to the simple CP pretreatment. On the other hand, use of CP alone for pretreatment provided the maximum electroactive Pt area relative to the other methods. This result may indicate the formation by CP of a population of oxygen-containing functional groups on the carbon surface different from that obtained with AP and one that is more favorable for anchoring the dendrimers. The differences in the chemistry of the surfaces were examined by means of IR spectroscopy.

3.3 Surface characterization of the carbon-fiber electrodes

The nature of the superficial functional groups produced by each pretreatment method was investigated by infrared (IR) spectroscopy. Specular-reflectance IR measurements were carried out on the modified carbon-fiber surfaces using a Thermo Nicolet spectrophotometer provided with Omnic 32 software, Version 6.1. Spectra were taken with an incidence angle of 45° at four or more randomly selected points on each surface.

Figure 5a shows the IR spectra of untreated carbon-fiber electrodes and of those exposed to the pretreatments. It was found that the carbon-fibers pretreated in acidic media

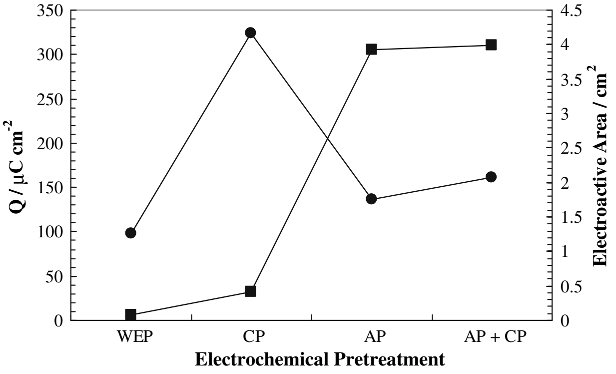

Fig. 4 Relationship between surface-charge density Q (■) and the electroactive area A_e (●) determined for the carbon-fiber surfaces according to each type of pretreatment used. CP indicates cyclic polarization, AP corresponds to anodic polarization. WEP is the unpretreated carbon-fiber included as a control

presented absorption bands at 1,660 and 1,710 cm^{-1}; these signals are attributed to IR absorption by quinone and carboxylic species, respectively [17, 49]. Furthermore, it was found that the surface pretreated by CP alone produced a much stronger signal at 1,660 cm^{-1}. This difference in peak intensity suggests that the CP treatment produces a relatively greater amount of quinone species on the surface of the carbon fibers. This conclusion is supported by the voltammetric response obtained with an unmodified carbon-fiber, curve *i* in Fig. 3, which exhibits a cathodic and the reverse anodic peak between 0.5 and 0.8 V (NHE) corresponding to the creation and destruction of quinone-like species [50–52].

Further IR results are shown in Fig. 5b, which compares the spectra of an unmodified CP-pretreated surface with one that had been subsequently modified with the Pt-dendrimer composite. These spectra reveal that the absorption band at 1,660 cm^{-1} is decreased considerably when the carbon-fiber was loaded with the G4OHPt. On the other hand, the band at 1,710 cm^{-1} associated with carboxylate species was not affected greatly. In the case of the carbon fibers pretreated by AP or AP + CP the decrease in the band located at 1,660 cm^{-1} was lower than with CP. This suggests that the oxidative activation of the carbon-fiber surface by CP alone promotes primarily the formation of quinone species on the electrode. According to Maeda and coworkers, such species favor the anchoring of hydroxyl-terminal dendrimer groups by means of an ether linkage [20–23].

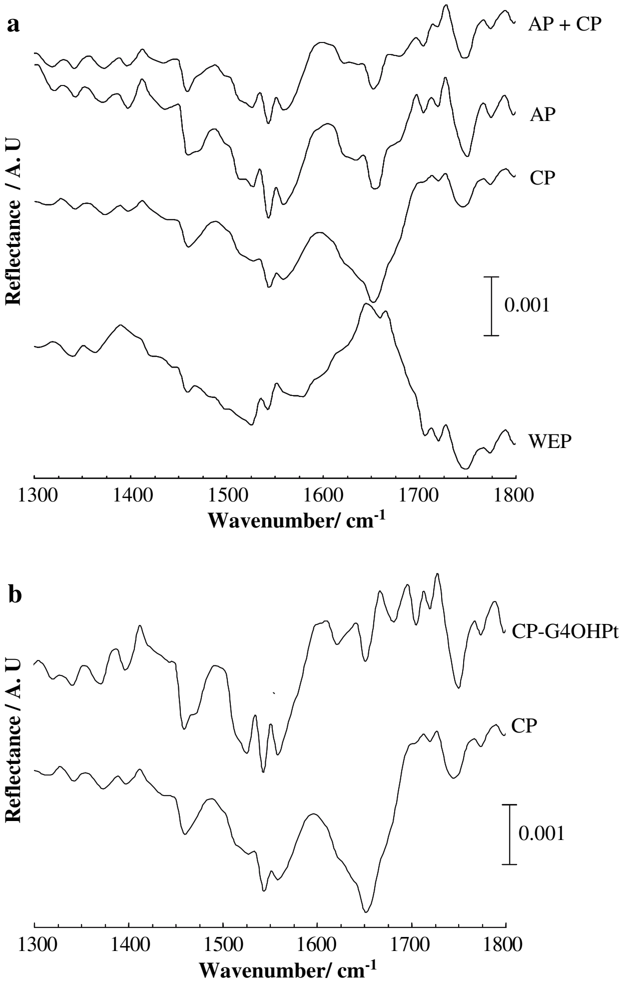

Fig. 5 (**a**) Specular-reflectance IR spectra of unpretreated (WEP) and pretreated carbon-fiber surfaces (CP, AP and AP + CP). (**b**) Comparison of the spectra of unmodified and of G4OHPt-modified carbon-fiber electrodes (both CP-functionalized)

It appears that the anodic polarization (AP) pretreatment produces a higher degree of surface oxidation of the carbon surface, generating several types of carboxylic, anhydride or lactone species [17–19], on which nucleophilic attack of hydroxyl-terminated dendrimer groups is not favored. On the basis of these results we identified CP alone as the electrochemical pretreatment of choice for the modification of the carbon-fiber electrodes with G4OHPt. Accordingly, that material was chosen for testing as an oxygen-reduction electrode.

3.4 Evaluation of the modified carbon-fiber electrode as an oxygen cathode

The kinetics parameters of the oxygen-reduction reaction (ORR) on the G4OHPt-modified carbon-fiber electrodes pretreated by CP, were determined by means of rotating disk electrode (RDE) polarization measurements. For these experiments, carbon-fiber disk electrodes were prepared from the Toray® carbon-fiber paper (0.19 mm thick), which was pasted onto a glassy-carbon disk substrate with conductive carbon paint (Spi®). This disk electrode was washed with HNO_3 (10%), rinsed, and dried. The surface was then functionalized by the CP pretreatment and modified with G4OHPt as described in Sect. 2.4. The RDE experiments were carried out at 5 rotation rates (between 100 and 900 rpm) in aqueous 0.5 M H_2SO_4 solution saturated with pure oxygen at 25 °C. The cathodic scan rate was 5 mV s^{-1}.

The catalytic activity of the G4OHPt-modified carbon-fiber surfaces for the ORR was compared with that of the bare carbon-fiber material. Figure 6 shows the polarization curves for O_2 reduction on a G4OHPt-modified carbon-fiber (a-*i*) and on a carbon-fiber surface (b), both surfaces previously pretreated by CP. It is clear in the figure that the modified electrode does catalyze oxygen reduction (Fig. 6a-*i*), exhibiting a half-wave potential $E_{1/2}$ of 0.65 V versus NHE approximately. The unmodified carbon-fiber electrode (Fig. 6b) presents at potentials 0.5–0.8 V only the response that corresponds to reduction of the quinone-like surface species, for which the current does not depend of the rotation rate. At more cathodic potentials (≤ 0.2 V) oxygen reduction is observed, but the current densities are much lower than those on the modified electrode. Figure 6 includes as a comparison the polarization curve for oxygen reduction on a commercial electrocatalyst (E-Tek® 30 wt% Pt/C) impregnated on glassy carbon electrode (a-*ii*).

Kinetics parameters (Tafel slope b and the exchange-current density J_0, based on superficial electrode area) were obtained from the modified-electrode polarization curves shown in Fig. 6a by means of a Koutecky–Levich analysis [53–57] according to the relation:

$$\frac{1}{J} = \frac{1}{J_k} + \frac{1}{J_D} \tag{1}$$

where J is the measured current density, J_K is the kinetic current density given by the cathodic Tafel expression

$$J_k = J_0 \exp(-b\eta) \tag{2}$$

where η is the overpotential, and J_D is the diffusion-limited current density, given by

$$J_D = 0.62nFD^{2/3}\omega^{1/2}\nu^{-1/6}C_{O_2} \tag{3}$$

The polarization data from Fig. 6a are plotted in Fig. 7 according to the form of Eq. 1. The current densities were based on the superficial area of the disk electrode, and the parameters for 0.5 M H_2SO_4 in Eq. 3 were taken to be an oxygen saturation concentration C_{o_2} of 1.1×10^{-6} mol cm^{-3} [58] and a diffusion coefficient D of 1.4×10^{-5} cm^2 s^{-1} [53]. The data were fitted with the value of n, the number of electrons involved in the reaction, set at 2 and at 4. It was found that the Koutecky–Levich slopes of our experimental data were about 0.39 mA cm^{-2} – (rad/s)$^{-1/2}$ while the theoretical values for $n = 4$ and $n = 2$ are 0.33 and 0.16, respectively. Thus, $n = 4$ fits the experimental data better, indicating an O_2-reduction process via the 4-electron pathway [59].

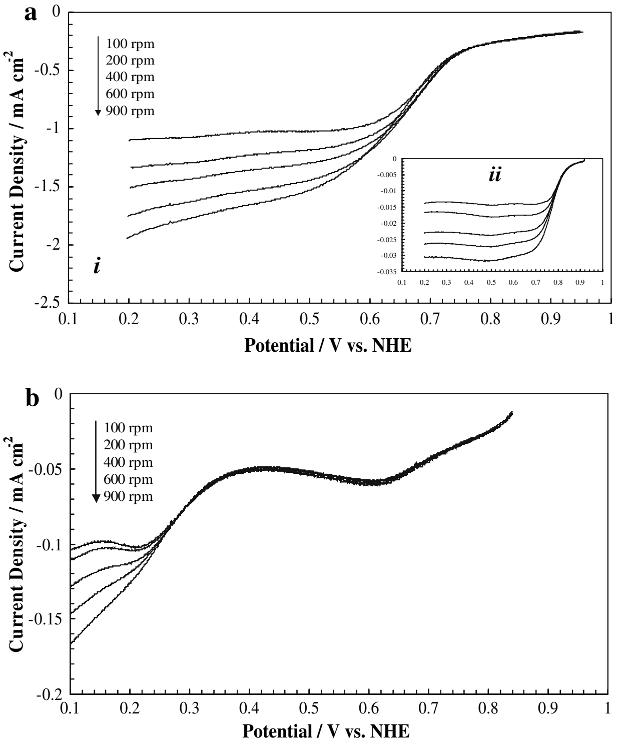

Fig. 6 Cathodic RDE voltammograms for the ORR at various rotation rates on (**a**-*i*) G4OHPt-modified, (**a**-*ii*) 30 wt% Pt/C and (**b**) unmodified carbon-fiber electrodes in O_2-saturated 0.5 M H_2SO_4. Scan rate: 5 mV s^{-1}

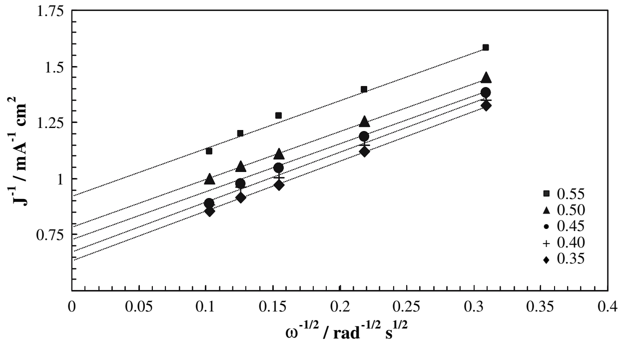

Fig. 7 Koutecky–Levich plots for the ORR on G4OHPt-modified carbon-fiber electrodes from the data of Fig. 6a-*i* taken at different values of potential

The values of the kinetics parameters obtained from a Tafel plot of the kinetic current densities obtained from the intercepts in Fig. 7 are shown in Table 1, along with the values of the open-circuit potential E_{OC} and $E_{1/2}$, for the G4OHPt-modified carbon-fiber electrode in 0.5 M H_2SO_4 saturated with O_2. Table 1 also presents the corresponding values for oxygen reduction obtained with a glassy-carbon electrode coated with a commercial E-Tek® composite of 30 wt% Pt/C nanoparticles [5, 60, 61]. The exchange-current density obtained with the modified carbon-fiber electrode, 3.3×10^{-7} mA cm^{-2}, is comparable to values reported for massive-platinum surfaces, e.g., 1.5×10^{-7} mA cm^{-2} [62, 63], but it is 75% lower than that for the E-Tek® nanoparticle catalyst, 15×10^{-7} mA cm^{-2}. On the other hand, the value of J_0 obtained with the dendrimer-supported Pt is achieved with only 12% as much electroactive area. It is notable also that the Tafel slope is higher for the modified carbon-fiber electrode, which indicates that the electrode presents less polarization at higher currents. Another factor to consider in comparing the two electrodes is the effect of diffusion in the porous carbon-fiber support. Diffusional effects can reduce the observed value of current compared to that which would be obtained if all of the Pt were exposed to an oxygen concentration equal to that at the outer surface of the porous layer.

Table 1 Oxygen-reduction kinetics parameters from the Koutecky–Levich analysis obtained with the G4OHPt-modified carbon-fiber electrode ($n = 4$) and for a commercial Pt-impregnated glassy-carbon electrode

Electrode	E_{oc}/V vs. NHE	$E_{1/2}$/V vs. NHE	b/V dec^{-1}	10^7 J_0/mA cm^{-2}	A_e	m_{Pt}/g cm^{-2}
G4OHPt-modified carbon-fiber	0.87	0.65	−0.130	3.3	14.8	14.2×10^{-6}
30 wt% Pt/C (E-Tek®)	0.98	0.82	−0.103	15	125.3	1.11×10^{-4}

Also given are the electroactive areas and platinum loadings of the two electrodes. Exchange-current density and Pt loading are based on the superficial electrode area

The platinum loading m_{Pt} (g cm^{-2}) on each type of electrode may be carbon-fiber and electrode was estimated with the equation given by Geniès and coworkers [64]. This calculation involves the average particle diameter d, estimated by means of XRD (2.7 nm), the Pt density ρ [65], and the electroactive area A_e of Pt nanoparticles supported by the PAMAM dendrimer. According to our results and to the value reported for E-Tek®, the Pt nanoparticles on both types of electrode are of roughly the same size. Thus the Pt-loading values should be proportional to the electroactive areas determined from hydrogen desorption. Estimated loading values, calculated with a particle diameter of 2.7 nm for the carbon-fiber material and 2.5 nm for the E-Tek® composite, are given in Table 1 along with the experimental values for A_e. area values for both cases were estimated from hydrogen desorption.

The results reveal that m_{Pt} on the G4OHPt-modified carbon-fiber electrode is smaller, by nearly 8 times, than that present on the commercial nanoparticle catalyst. Taking into account this difference in Pt loading, it appears that the true exchange current density on the platinum surface is 70% higher for the Pt supported by dendrimer. This result might be attributed to the local chemical environment established by the dendrimers or to the predominance of oxidized species on the pretreated carbon-fibers, which could contribute some alteration in the ORR mechanism. Finally, it is noted that the results shown here were reproducible in replicated experiments run after the modified carbon-fiber electrode was left in water for several days; thus, the surfaces were stable.

4 Conclusions

In summary, we have described the preparation and characterization of carbon-fiber-paper electrodes with electrocatalytic surfaces based on platinum nanoparticles supported by PAMAM dendrimers. Anodic pretreatment of the substrate in acidic media, specifically by means of cyclic polarization (CP), facilitated the immobilization of the metallic nanocomposites prepared in solution from a Pt salt and monodisperse macromolecular dendrimers, which serve as nanoreactors for the synthesis of encapsulated nanoparticles. This interesting electrode concept offers a promising approach for the development of electrocatalytic surfaces for application in fuel-cell technology because good catalytic activity for oxygen reduction can be obtained with metal loadings lower than those used by currently available commercial catalysts. Based on the good performance of the new electrode material when expressed on the basis of the mass of Pt used, there exists an opportunity to produce superior catalytic electrodes if higher loadings of the dendrimer-Pt composite can be achieved.

Acknowledgments The authors gratefully acknowledge financial support from the Mexican Council for Science and Technology (CONACyT, Grant 45157). We also thank CNR-ITAE Institute (Messina, Italy) for support with the XRD and SEM measurements. JLG also acknowledges CONACyT for a graduate fellowship. TWC is a Cooperante supported by U. S. Peace Corps under agreement with CONACyT.

References

1. Kinoshita K (1988) Carbon, electrochemical and physicochemical properties. Wiley, New York
2. McCreery RL (1991) In: Bard Allen J (eds) Electroanalytical chemistry, vol. 17. Marcel Dekker, New York
3. Kokhanov GN, Milova NG (1989) In: Conway BE, Bockris J, White PE (eds) Modern aspects of electrochemistry, vol. 20. Plenum Press, New York
4. McDermott MT, Kneten K, McCreery RL (1992) J Phys Chem 96:3124
5. Benítez R, Chaparro AM, Daza L (2005) J Power Sources 151:2
6. Cui H-F, Ye J-S, Zhang W-D, Wang J, Sheu F-S (2005) J Electroanal Chem 577:295
7. Guo JW, Zhao TS, Prabhuram J, Wong CW (2005) Electrochim Acta 50:1973
8. Vaik K, Sarapuu A, Tammeveski K, Mirkhalaf F, Schiffrin DJ (2004) J Electroanal Chem 564:159
9. Ishifune M, Suzuki R, Mima Y, Uchida K, Yamashita N, Kashimura S (2005) Electrochim Acta 51:14
10. Ledesma J, Escalante IL, Chapman TW, Rodríguez FJ, Godínez LA (2006) The electrochemical society proceedings series, Cancun Mex. ECS Trans 3:7
11. Dekanski A, Stevanović J, Stevanović R, Nikolić BŽ, Jovanović VM (2001) Carbon 39:1195
12. Lakshminarayanan PV, Toghiani H, Pittman CU (2004) Carbon 42:2433
13. Basova YV, Hatori H, Yamada Y, Miyashita K (1999) Electrochem Commun 1:540
14. Pittman CU, Jiang W, He G-R, Gardnar SD (1998) Carbon 36:25
15. Gulyás J, Földes E, Lázár A, Pukánszky B (2001) Compos Part A 32:353

16. Sullivan MG, Schnyder B, Bartsch M, Alliata D, Barbero C, Imhof R, Kotz R (2000) J Electrochem Soc 147:2636
17. Yang Y, Lin G (1995) J Appl Electrochem 25:259
18. Jovanović VM, Terzić S, Tripković AV, Popović K Dj, Lović JD (2004) Electrochem Commun 6:1254
19. Kiema G, Aktay M, McDermott M (2003) J Electroanal Chem 540:7
20. Maeda H, Yamauchi Y, Hosoe M, Li T-X, Yamaguchi E (1994) Chem Pharm Bull 42:1870
21. Maeda H, Itami M, Yamauchi Y, Ohmori H (1996) Chem Pharm Bull 44:2294
22. Maeda H, Katayama K, Matsui R, Yamauchi Y, Ohmori H (2000) Anal Sci 16:293
23. Maeda H, Saka-Iri Y, Ogasawara T, Huano CZ, Yamauchi Y, Ohmori H (2001) Chem Pharm Bull 49:1349
24. Ye H, Crooks RM (2005) J Am Chem Soc 127:4930
25. Ye H, Crooks RM (2007) J Am Chem Soc 129:3627
26. Zhao M, Sun L, Crooks RM (1998) J Am Chem Soc 120:4877
27. Balogh L, Tomalia DA (1998) J Am Chem Soc 120:7355
28. Zhao M, Crooks RM (1999) Adv Mater 11:217
29. Zhao M, Crooks RM (1999) Chem Mater 11:3379
30. Chung YM, Rhee HK (2003) Catal Lett 85:159
31. Scott RW, Datye AK, Crooks RM (2003) J Am Chem Soc 123:3708
32. Lang H, May Alan R, Iversen BL, Chandler BD (2003) J Am Chem Soc 125:14832
33. Vijayaraghavan G, Stevenson K (2007) Langmuir 23:5279
34. Lee JW, Popov B (2007) J Solid State Electrochem 11:1355
35. Crooks RM, Zhao M, Sun L, Chechik V, Yeung LK (2001) Acc Chem Res 34:181
36. Liu D, Gao J, Murphy CJ, Williams CT (2004) J Phys Chem B 108:12911
37. Xie H, Gu Y, Ploehn H (2005) Nanotechnology 16:S492
38. Crespilho FN, Huguenin F, Zucolotto V, Olivi P, Nart FC, Oliveira ON (2006) Electrochem Commun 8:348
39. Murthi VS, Urian RC, Mukerjee S (2004) J Phys Chem B 108:11011
40. Centeno TA, Stoeckli F (2006) J Power Sources 154:314
41. Anh H-J, Sohn JI, Kim Y-S, Shim H-S, Kim W-B, Seong T-Y (2007) Electrochem Commun 8:513
42. Biegler T, Rand DAJ, Woods R (1971) J Electroanal Chem 29:269
43. Hsueh K-L, Gonzalez ER, Srinivasan S (1983) Electrochim Acta 5:691
44. Sawyer Donald T, Sobkowiak A, Roberts JL (1995) Electrochemistry for chemists. John Wiley, New York
45. Sarapuu A, Vaik K, Schiffrin DJ, Tammeveski K (2003) J Electroanal Chem 541:23
46. Trasatti S, Petri OA (1992) J Electroanal Chem 327:353
47. Schmidt TJ, Gasteiger HA, Stäb GD, Urban PM, Kolbe DM, Behm RJ (1998) J Electrochem Soc 145:2354
48. Rodriguez DJM, Melían JAH, Peña JP (2000) J Chem Edu 9:1195
49. Gregoriou GV, Rodman ES (2002) In: Chalmers John M, Griffiths Peter R (eds) Handbook of vibrational spectroscopy, vol 4. Wiley, New York
50. Bard Allen J (1978) In: Encyclopedia of electrochemistry of the elements, organic section, vol XII. Marcel Dekker, New York
51. Diaz AF (1991) In: Lund Henning, Baizer Manuel M (eds) Organic electrochemistry, an introduction and a guide. Marcel Dekker, New York
52. Sarapuu A, Vaik K, Schiffrin DJ, Tammeveski K (2003) J Electroanal Chem 541:23
53. El-Deab Mohamed S, Osaka Takeo (2002) Electrochim Acta 47:4255
54. Baranton S, Coutanceau C, Roux C, Hahn F, Léger J-M (2005) J Electroanal Chem 577:223
55. Maruyama Jun, Abe Ikuo (2002) J Electroanal Chem 527:65
56. Gileadi E (1993) Electrode kinetics for chemists, chemical engineers and materials scientists. Wiley-VCH, New York
57. Bard Allen J, Faulkner L (1980) Electrochemical methods. Wiley, New York
58. Jakobs RCM, Janssen LJ, Barendrecht E (1985) Electrochim Acta 30:1085
59. Yeager E (1984) Electrochim Acta 29:1527
60. Antolini E, Passos R, Ticianelli E (2002) Electrochim Acta 48:263
61. Higuchi E, Uchida H, Watanabe M (2005) J Electroanal Chem 583:69
62. Kinoshita K (1992) Electrochemical Oxygen technology. Wiley, New York
63. Jiang J, Yi B (2005) J Electroanal Chem 577:107
64. Geniès L, Faure R, Durand R (1998) Electrochim Acta 44:1317
65. Duarte MME, Pilla AS, Sieben JM, Mayer CE (2006) Electrochem Commun 8:159